Thiol-Anchored TIPS-Tetracene Ligands with Quantitative Triplet Energy Transfer to PbS Quantum Dots and Improved Thermal Stability

Victor Gray†,‡, Zhilong Zhang†, Simon Dowland†, Jesse R. Allardice†, Antonios M. Alvertis†, James Xiao†, Neil C. Greenham†, John E. Anthony||, Akshay Rao†**

†Cavendish Laboratory, University of Cambridge, J. J. Thomson Avenue, Cambridge CB3 0HE, U.K.

‡Department of Chemistry - Ångström Laboratory, Uppsala University, Box 523, 751 20, Uppsala, Sweden.

||University of Kentucky Center for Applied Energy Research, 2582 Research Park Drive, Lexington Kentucky 40511, United States.

Corresponding Author

*corresponding author email: ar525@cam.ac.uk, anthony@uky.edu

ABSTRACT: Triplet energy transfer between inorganic quantum dots (QDs) and organic materials plays a fundamental role in many optoelectronic applications based on these nanocomposites. Attaching organic molecules to the QD as transmitter ligands has been shown to facilitate transfer both to and from QDs. Here we show that the often disregarded thiol anchoring group can achieve quantitative triplet energy transfer yields in a PbS QD system with 6,11-bis((triisopropylsilyl)ethynyl) tetracene-2-methylthiol (**TET-SH**) ligands. We demonstrate efficient triplet transfer in a singlet-fission-based photon multiplication system with 5,12-bis((triisopropylsilyl)ethynyltetracene (**TIPS-Tc**) generating triplets in solution which transfer to the PbS QDs *via* the thiol ligand **TET-SH**. Importantly, we demonstrate increased thermal stability of the PbS-**TET-SH** system, compared to the traditional carboxylic acid counterpart, allowing for higher photoluminescence quantum yields.

TOC GRAPHICS

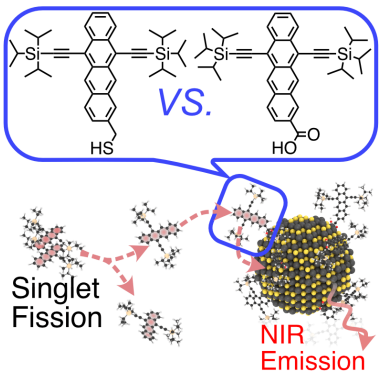

KEYWORDS triplet energy transfer, singlet fission, quantum dots, photon multiplication, thiol ligands

Quantum dot-organic nanocomposites are optoelectronic materials with both organic semiconductor molecules and quantum dots (QDs) as counterparts. Ideally these nanocomposites are able to harness the advantage of both classes of materials to tailor the material's properties for specific applications.[1] With almost unlimited possible materials combinations many fields have come to exploit these types of nanocomposites, including photocatalysis,[2,3] bioimaging and sensing,[4] solar energy harvesting and photon upconversion,[5,6] light-emitting diodes[5] and, recently, singlet-fission-based photon multiplication.[7-9] The choice of the organic and inorganic counterparts will depend on the desired use of the nanocomposite, *i.e.* charge transfer, energy transfer or photon emission will require different QD-organic combinations.

Since organic molecules have relatively large singlet-triplet splitting and small spin-orbit coupling the interconversion between singlets and triplet states is inefficient. In QDs on the other hand, spin-orbit coupling is large and spin states can be separated by less than 10 meV.[1,10,11] QDs can therefore act as "spin-mixers" in QD-organic nanocomposites.[12] These "spin-mixing" materials have gained significant attention as triplet sensitizers for photon upconversion applications, and recently as "triplet" emitters in singlet-fission-based photon multiplication. In such systems, an organic molecule is attached to the QD as a ligand, and serves to either transfer triplet energy into, or receive it from, the QD. The choice of ligand is crucial in such QD-ligand systems and must fulfill two main requirements. Firstly, triplet energy transfer from or to the QD must be efficient. Secondly, the ligand must be stably bound on the QD, otherwise the composite system will fall apart in time.

Singlet fission is a spin- and energy-conserving exciton multiplication process in organic semiconductors that splits a singlet excited state to two triplet excited states.[7,13] As an exciton multiplication process, it has been proposed as a means to overcome thermalization losses in photovoltaic (PV) devices and surpass the Shockley-Queisser limit.[7,13] There are two main approaches to integrate singlet fission materials with PVs: either direct integration, where the singlet fission material transfers the electrons or excitons directly to the PV material,[14–16] or a photon multiplication integration where the generated triplets are first transferred to an emitting material, *e.g.* QDs, which re-emits the exciton energy as photons for the PV to absorb, effectively converting the exciton process to a photon multiplication process.[7–9,17] The first approach might at first appear to be a simpler integration method, however, since its suggestion 40 years ago[14] many challenges remain. We have recently demonstrated the feasibility and limitations of the photon multiplication system.[8,9] Crucial for a singlet-fission-based photon multiplication system is efficient triplet transfer from the organic singlet fission material to the inorganic QDs. To achieve efficient triplet transfer the QD is covered by a triplet transmitter ligand.[8] The transmitter ligand should enable efficient coupling between the QD and the ligand without introducing parasitic excited state deactivation pathways and traps. In this way the QD-organic ligand system for photon multiplication is very similar to that used for triplet-sensitized triplet-triplet annihilation (TTA) photon upconversion and much can be learned from these well-studied systems.[18–22] Based on the many studies of CdSe QD-ligand systems it has been concluded that ligands anchored with thiols, even though more strongly bound, are undesirable as they result in intramolecular or interfacial charge transfer events competing with the desired triplet energy transfer and photon emission events.[21,23–27] This assumption, that thiols introduce charge transfer pathways could explain the lack of reports of thiol anchored ligands used for QD-organic

nanocomposites designed for triplet energy transfer. However, we note that for other QD materials, such as CdTe and PbS there are reports of thiol anchored ligands that do not quench the QD photoluminescence (PL).[23,28–30]

We therefore chose to investigate a thiol-anchored TIPS-tetracene ligand as a triplet transmitter ligand for PbS QDs. We establish that the *a priori* disregarding of thiol-anchored ligands for triplet energy transfer reactions should be reconsidered. By comparing the 6,11-bis((triisopropylsilyl)ethynyl)tetracene-2-carboxylic acid (**TET-CA**) ligand with a thiol counterpart 6,11-(bis((triisopropylsilyl)ethynyl)tetracen-2-yl)methanethiol (**TET-SH**) in a solution-based photon multiplication system[8,9] we demonstrate that the thiol-anchored ligand allows for equally efficient triplet energy transfer to the PbS QD. Triplet energy transfer from the singlet fission materials in solution to the ligand and subsequent transfer from the ligand to PbS QDs approaches 100% efficiency with both carboxylic acid and thiol ligands. Furthermore, we demonstrate the advantage of using a stronger-binding thiol anchor as the thermal stability of the QD-organic nanocomposite distinctly improves.

We recently developed a singlet-fission-based photon multiplication system in solution.[8] The photon multiplication process is schematically described in Figure 1. It consists of a highly soluble singlet fission material, 5,12-bis((triisopropylsilyl)ethynyl)tetracene (**TIPS-Tc**) and PbS QDs with triplet transmitter ligands attached. **TIPS-Tc** undergoes singlet fission in concentrated solution generating triplet excitons with approximately 130% yield.[8,9,31] The triplets are transferred *via* the transmitter ligand to the PbS QDs, which subsequently emits an NIR photon when returning to the ground state. If triplet transfer is inefficient or does not occur, as is the case without transmitter ligands,[8] no or inefficient NIR emission from the QDs is observed. Therefore, by measuring the photoluminescence quantum efficiency (PLQE) of the QDs when exciting the

QDs directly (658 nm) and comparing to when exciting the singlet fission material **TIPS-Tc** (515 nm) we can obtain a direct measure of the triplet transfer efficiency. We therefore choose this system as a straightforward way to evaluate a new triplet transmitter ligand (6,11-bis((triisopropylsilyl)ethynyl)tetracen-2-yl)methanethiol (**TET-SH**) containing a thiol anchoring group and compare it to the carboxylic acid counterpart (**TET-CA**), Figure 1a.

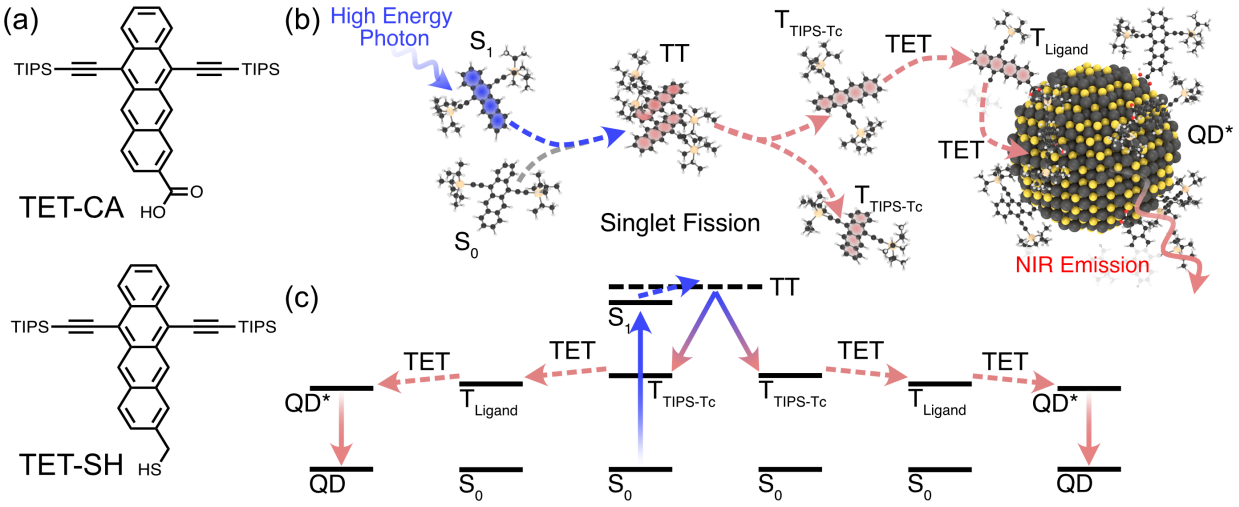

Figure 1. (a) Structures of the triplet transmitter ligands **TET-CA** and **TET-SH**. (b) Schematic illustration of the singlet-fission-based photon multiplication process in solution. First, a high-energy photon is absorbed by **TIPS-Tc** to form its first singlet excited state S_1. Together with a ground-state molecule singlet fission proceeds *via* an intermediate triplet pair state (TT) to form two independent triplets. Triplet energy transfer (TET) occurs from **TIPS-Tc** to a transmitter ligand followed by another TET step to populate the QD excited state (QD*) from which a NIR photon is emitted. (c) The photon multiplication process in (b) described in a Jablonski diagram.

Ligand exchange of PbS QDs with bandgaps ranging from 1.0 – 1.3 eV was performed following a similar procedure to that we have reported previously for **TET-CA**,[9] resulting in similar ligand

coverage for both **TET-CA** and **TET-SH** ligands on the PbS QDs (see Supporting Information and Figure S1 for more details).

After ligand exchange, the QD intrinsic PLQE slightly drops for QDs with bandgaps smaller than 1.1 eV, Figure 2. This minor drop was observed previously for **TET-CA** ligated PbS QDs with similar bandgaps and was ascribed to trap quenching from traps introduced during the ligand exchange.[9] For QDs with bandgaps close to or higher than the triplet energy of the ligand (T_{Ligand} ~1.2 eV) the PL is quenched more substantially, as triplet transfer from the QD to the ligand becomes possible. A blue shift of the QD peak absorption and a minor red shift of the ligand absorption is also observed after ligand exchange. Similar spectral shifts are commonly observed in QD-ligand nanocomposites and can arise due to the electronic interactions between the ligand and QD. [32–34]

Dissolving the **TET-SH** ligated QDs in concentrated **TIPS-Tc** toluene solutions produces a photon multiplication system where the TIPS-Tc singlet fission material functions as the excition multiplication material and the ligand covered QDs are the emitters. Figure 2a compares the QD PL response when exciting either the QD directly (658 nm) or exciting mainly the **TIPS-Tc** singlet fission material (515 nm). We note that approximately 95% of incoming photons are absorbed by **TIPS-Tc**.[8] It is clear that there is an enhancement of the QD PLQE when **TIPS-Tc** is excited. Assuming that the enhancement is due to singlet fission followed by triplet transfer to the QD, as we have shown previously for **TET-CA** ligated QDs,[8,9] the number of transferred triplets per absorbed photon (η_T) can be calculated from Equation 1.[8,9,35]

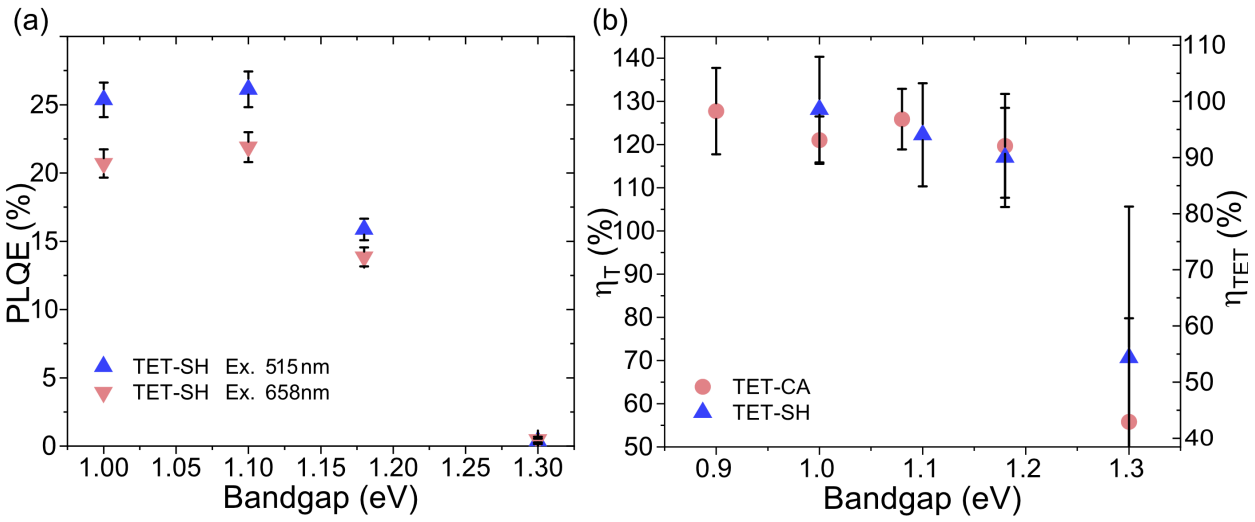

Figure 2. (a) Photoluminescence quantum efficiency (PLQE) of PbS quantum dots of different bandgap after ligand exchange to **TET-SH** in a toluene solution with 200 mg/mL **TIPS-Tc**, exciting the QDs directly (658 nm) or the singlet fission material **TIPS-Tc** (515 nm). QD concentrations are 0.2 mM. (b) Triplet transfer efficiency per absorbed photon (η_T, left axis) and internal triplet transfer efficiency (η_{TET}, right axis), calculated from the PLQE enhancement in (a) compared to the triplet transfer efficiency of **TET-CA** ligated dots.

$$\eta_T = \left(\frac{\Phi_{PM}}{\Phi_{QD}} - \frac{Abs_{QD}^{515\,nm}}{Abs_{Tot}^{515\,nm}}\right)\left(\frac{Abs_{TIPS-Tc}^{515\,nm}}{Abs_{Tot}^{515\,nm}}\right)^{-1} = \eta_{SF}\eta_{TET}. \quad (1)$$

Here Φ_{PM} and Φ_{QD} are the measured PLQE values when exciting the singlet fission material TIPS-Tc and the QD, respectively. $Abs_{Tot}^{515\,nm}$ is the total absorption at the excitation wavelength affording photon multiplication, here 515 nm. The total absorption is the sum of the absorption of the two components; TIPS-Tc ($Abs_{TIPS-Tc}^{515\,nm}$) and the QDs ($Abs_{QD}^{515\,nm}$). η_{SF} and η_{TET} are the singlet fission quantum yield and the internal triplet transfer efficiency, respectively.

We recently showed that η_T is 120±10 % for **TET-CA** ligated QDs for bandgaps below 1.25 eV.[8,9] In Figure 2b we compare η_T for QDs with **TET-SH** ligands to the case with **TET-CA** ligands. It

is evident that both the carboxylic acid- and thiol-anchored ligands allow for equally efficient triplet transfer. Considering that the singlet fission triplet yield (η_{SF}) in concentrated **TIPS-Tc** solutions is 130±10 %, the internal triplet transfer efficiency (η_{TET}) is close to unity for QDs with bandgaps below 1.2 eV, Figure 2b.

We also investigate the possibility for charge transfer pathways by comparing the energetic alignment of the ligand HOMOs and the PbS QDs valance band, Figure 3. From UPS and cyclic voltammetry (CV) measurements, the conduction band of PbS QDs of similar bandgaps to those studied here have been reported to be in the interval -4.9 eV to -5.1 eV *vs*. vacuum.[36–40] From CV measurements we determine the HOMO level of **TIPS-Tc** to be -5.5 eV. The relative change of the ligand ionization potential is estimated from DFT calculations. The orbital energies of the three molecules were calculated based on density functional theory, at the B3LYP/cc-pVDZ level of theory, using the NWChem software.[41] Relative to **TIPS-Tc** the HOMO for **TET-SH** is practically unchanged (+0.01 eV). The ligand **TET-CA** shifts to more negative potentials by less than 0.2 eV. The triplet energy of these tetracene derivatives is about 1.25 eV.[9] Based on these calculations hole transfer is more likely for the **TET-CA** ligand. However, in our previous work, we did not find any indication of hole transfer or hole transfer mediated triplet transfer for the PbS/**TET-CA** system, suggesting that hole transfer is not an issue for the PbS/**TET-SH** system either.[8,9] We note that the band alignment also indicates that triplet energy transfer from a higher energy (>1.25 eV) QD to either ligand **TET-SH** or **TET-CA** ligand is not mediated by charge transfer.[22] Hole trapping due to surface states introduced by the ligand cannot be ruled out by this simple band alignment argument. With close to quantitative triplet transfer, however, hole trapping is not likely to be an issue for the **TET-SH** ligand.

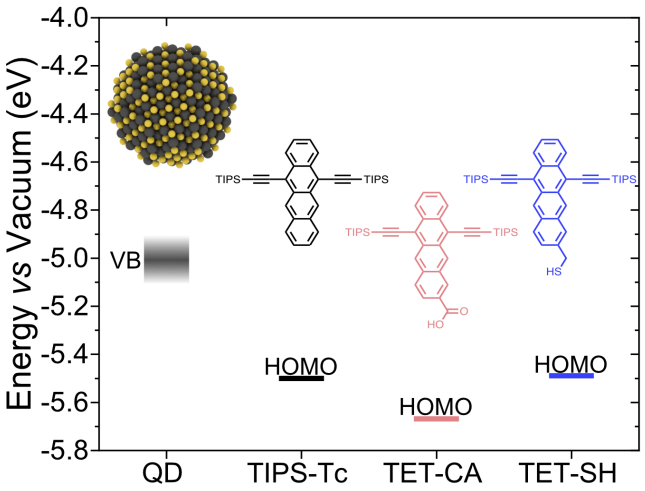

Figure 3. Band alignment *vs* vacuum of PbS QD valance band edge (range -5.1 to -4.9 eV from literature) compared to the HOMO of **TIPS-Tc** (from cyclic voltammetry) and the HOMO of the ligands **TET-CA** and **TET-SH** (relative difference *vs* **TIPS-Tc** from DFT calculations).

The advantage of using thiol-anchored ligands is arguably the stronger binding affinity to chalcogenide QDs.[21,42] Binding affinity can be particularly important when considering future processing and commercialization of applications as it may limit process parameters such as temperature and solvent. To illustrate the advantage of using a thiol linker we measured the PbS QD intrinsic PL of 1.1 eV QDs with oleic acid, **TET-CA** and **TET-SH** before and after heating the liquid samples to 100 °C for 1 h and 32 h. As seen in Figure 4 the **TET-SH** capped PbS QDs retain their PL even after 32 h heating, whereas the **TET-CA** capped QDs lose over 30% of their PL intensity. We hypothesize that the PL drop is due to ligand loss, since it is accompanied by an increase in emission from the ligand when exciting at 515 nm, indicative of more unbound ligand. We also note that there is only a minor redshift in the peak position (<25 nm) of the QD

PL after heating (Figure S4), indicating any change in QD size due to surface etching or QD fusion was minimal, <0.1 nm.

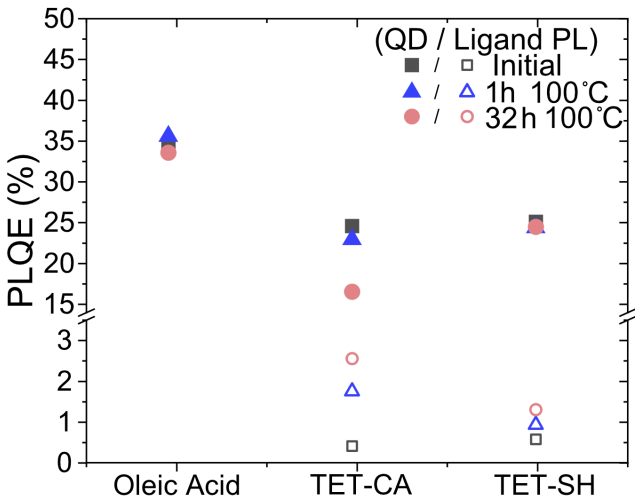

Figure 4. Photoluminescence quantum efficiency (PLQE) of PbS QDs capped with oleic acid, **TET-CA** or **TET-SH** ligands in toluene, before and after heating the samples to 100 °C. Also shown is the PLQE for the ligand emission. Excitation at 515 nm, 0.8 mW/cm^2, excites the QD and ligand simultaneously.

To conclude, we have shown that a thiol-anchored TIPS-tetracene ligand attached on PbS QDs functions as an efficient triplet transfer ligand. We also show that the stronger binding afforded by the thiol group leads to an improved thermal stability compared to the traditional carboxylic acid anchored ligand and therefore to higher photoluminescence quantum yields in photon multiplication based applications. Thiol-anchored active ligands have previously been disregarded for applications requiring triplet energy transfer due to possible hole trapping.[21,23] However, our results unambiguously demonstrate that hole trapping is not necessarily an issue

and that there are benefits when using a stronger-binding ligand. Recent work has shown that the relative band alignment of the ligand and QD governs the possibility of charge transfer and triplet energy transfer in this type of nanocomposite.[22] It has also been shown that the band alignment of PbS QDs can be tuned by varying the thiol ligand composition,[37] which might complicate the choice of thiol ligands. However, we argue that thiol ligands can be good candidates for mediating triplet energy transfer as long as the band alignment is kept to favor triplet transfer. Our findings are relevant for both photon upconversion and photon multiplication materials as well as general QD-organic nanocomposite materials for other optoelectronic applications.

ASSOCIATED CONTENT

Supporting information is available online with additional experimental details and data for the synthesis and ligand exchange of the QDs, calculation of QD ligand coverage and size distribution.

Data underlying the figures and conclusions in this publication is available at the University of Cambridge data repository at: link to be added during proof

AUTHOR INFORMATION

The authors declare no competing financial interests.

ACKNOWLEDGMENT

We thank the Winton Programme for the Physics of Sustainability and the Engineering and Physical Sciences Research Council for funding. This project has received funding from the European Research Council (ERC) under the European Union's Horizon 2020 research and innovation programme (grant agreement No 758826). VG acknowledges funding from the

Swedish research council, Vetenskapsrådet 2018-00238. J. R. A. acknowledges Cambridge Commonwealth European and International Trust for financial support. Z. Z. acknowledges funding from the European Union's Horizon 2020 research and innovation programme under the Marie Skłodowska-Curie Actions grant (No. 842271 – TRITON project). J. X. acknowledges EPSRC Cambridge NanoDTC, EP/L015978/1 for financial support. A.M.A. acknowledges the support of the Engineering and Physical Sciences Research Council (EPSRC) for funding under grant EP/L015552/1. JEA's materials synthesis was supported by the U.S. National Science Foundation under Cooperative Agreement No. 1849213.

REFERENCES

(1) Steiner, A. M.; Lissel, F.; Fery, A.; Lauth, J.; Scheele, M. Prospects of Coupled Organic-Inorganic Nanostructures for Charge and Energy Transfer Applications. *Angew. Chemie Int. Ed.* **2020**, DOI: 10.1002/anie.201916402. https://doi.org/10.1002/anie.201916402.

(2) Harris, R. D.; Bettis Homan, S.; Kodaimati, M.; He, C.; Nepomnyashchii, A. B.; Swenson, N. K.; Lian, S.; Calzada, R.; Weiss, E. A. Electronic Processes within Quantum Dot-Molecule Complexes. *Chem. Rev.* **2016**, *116* (21), 12865–12919. https://doi.org/10.1021/acs.chemrev.6b00102.

(3) Jiang, Y.; Wang, C.; Rogers, C. R.; Kodaimati, M. S.; Weiss, E. A. Regio- and Diastereoselective Intermolecular [2+2] Cycloadditions Photocatalysed by Quantum Dots. *Nat. Chem.* **2019**, *11* (11), 1034–1040. https://doi.org/10.1038/s41557-019-0344-4.

(4) Medintz, I. L.; Uyeda, H. T.; Goldman, E. R.; Mattoussi, H. Quantum Dot Bioconjugates for Imaging, Labelling and Sensing. *Nat. Mater.* **2005**, *4* (6), 435–446. https://doi.org/10.1038/nmat1390.

(5) Voznyy, O.; Sutherland, B. R.; Ip, A. H.; Zhitomirsky, D.; Sargent, E. H. Engineering

Charge Transport by Heterostructuring Solution-Processed Semiconductors. *Nat. Rev. Mater.* **2017**, *2*, 17026. https://doi.org/10.1038/natrevmats.2017.26.

(6) Wen, S.; Zhou, J.; Schuck, P. J.; Suh, Y. D.; Schmidt, T. W.; Jin, D. Future and Challenges for Hybrid Upconversion Nanosystems. *Nat. Photonics* **2019**, *13* (12), 828–838. https://doi.org/10.1038/s41566-019-0528-x.

(7) Rao, A.; Friend, R. H. Harnessing Singlet Exciton Fission to Break the Shockley-Queisser Limit. *Nat. Rev. Mater.* **2017**, *2*, 17063. https://doi.org/10.1117/2.1201203.004146.

(8) Allardice, J. R.; Thampi, A.; Dowland, S.; Xiao, J.; Gray, V.; Zhang, Z.; Budden, P.; Petty, A. J.; Davis, N. J. L. K.; Greenham, N. C.; et al. Engineering Molecular Ligand Shells on Quantum Dots for Quantitative Harvesting of Triplet Excitons Generated by Singlet Fission. *J. Am. Chem. Soc.* **2019**, *141*, 12907–12915. https://doi.org/10.1021/jacs.9b06584.

(9) Gray, V.; R. Allardice, J.; Zhang, Z.; Dowland, S.; Xiao, J.; J. Petty, A.; E. Anthony, J.; C. Greenham, N.; Rao, A. Direct vs Delayed Triplet Energy Transfer from Organic Semiconductors to Quantum Dots and Implications for Luminescent Harvesting of Triplet Excitons. *ACS Nano* **2020**, 10.1021/acsnano.9b09339. https://doi.org/10.1021/acsnano.9b09339.

(10) Scholes, G. D.; Rumbles, G. Excitons in Nanoscale Systems: Fundamentals and Applications. *Nat. Mater.* **2006**, *5* (September), 683–696. https://doi.org/10.1038/nmat1710.

(11) Scholes, G. D. Controlling the Optical Properties of Inorganic Nanoparticles. *Adv. Funct. Mater.* **2008**, *18* (8), 1157–1172. https://doi.org/10.1002/adfm.200800151.

(12) Nienhaus, L.; Wu, M.; Bulović, V.; Baldo, M. A.; Bawendi, M. G. Using Lead Chalcogenide Nanocrystals as Spin Mixers: A Perspective on near-Infrared-to-Visible

Upconversion. *Dalt. Trans.* **2018**. https://doi.org/10.1039/C8DT00419F.

(13) Smith, M. B.; Michl, J. Singlet Fission. *Chem. Rev.* **2010**, *110* (11), 6891–6936. https://doi.org/10.1021/cr1002613.

(14) Dexter, D. L. Two Ideas on Energy Transfer Phenomena: Ion-Pair Effects Involving the OH Stretching Mode, and Sensitization of Photovoltaic Cells. *J. Lumin.* **1979**, *18–19*, 779–784. https://doi.org/10.1016/0022-2313(79)90235-7.

(15) MacQueen, R.; Liebhaber, M.; Niederhausen, J.; Mews, M.; Gersmann, C.; Jäckle, S.; Jäger, K.; Tayebjee, M.; Jehangir, Y.; Schmidt, T. W.; et al. Crystalline Silicon Solar Cells with Tetracene Interlayers: The Path to Silicon-Singlet Fission Heterojunction Devices. *Mater. Horizons* **2018**, *5*, 1065–1075. https://doi.org/10.1039/C8MH00853A.

(16) Einzinger, M.; Wu, T.; Kompalla, J. F.; Smith, H. L.; Perkinson, C. F.; Nienhaus, L.; Wieghold, S.; Congreve, D. N.; Kahn, A.; Bawendi, M. G.; et al. Sensitization of Silicon by Singlet Exciton Fission in Tetracene. *Nature* **2019**, *571* (7763), 90–94. https://doi.org/10.1038/s41586-019-1339-4.

(17) Futscher, M. H.; Rao, A.; Ehrler, B. The Potential of Singlet Fission Photon Multipliers as an Alternative to Silicon-Based Tandem Solar Cells. *ACS Energy Lett.* **2018**, *3* (10), 2587–2592. https://doi.org/10.1021/acsenergylett.8b01322.

(18) Huang, Z.; Li, X.; Mahboub, M.; Hanson, K. M.; Nichols, V. M.; Le, H.; Tang, M. L.; Bardeen, C. J. Hybrid Molecule-Nanocrystal Photon Upconversion Across the Visible and Near-Infrared. *Nano Lett.* **2015**, *15* (8), 5552–5557. https://doi.org/10.1021/acs.nanolett.5b02130.

(19) Mongin, C.; Garakyaraghi, S.; Razgoniaeva, N.; Zamkov, M.; Castellano, F. N. Direct Observation of Triplet Energy Transfer from Semiconductor Nanocrystals. *Science* **2016**,

351 (6271), 369–372. https://doi.org/10.1126/science.aad6378.

(20) Mongin, C.; Moroz, P.; Zamkov, M.; Castellano, F. N. Thermally Activated Delayed Photoluminescence from Pyrenyl-Functionalized CdSe Quantum Dots. *Nat. Chem.* **2018**, *10* (December), 225–230. https://doi.org/10.1038/nchem.2906.

(21) Huang, Z.; Tang, M. L. Designing Transmitter Ligands That Mediate Energy Transfer between Semiconductor Nanocrystals and Molecules. *J. Am. Chem. Soc.* **2017**, *139* (28), 9412–9418. https://doi.org/10.1021/jacs.6b08783.

(22) Luo, X.; Han, Y.; Chen, Z.; Li, Y.; Liang, G.; Liu, X.; Ding, T.; Nie, C.; Wang, M.; Castellano, F. N.; et al. Mechanisms of Triplet Energy Transfer across the Inorganic Nanocrystal/Organic Molecule Interface. *Nat. Commun.* **2020**. https://doi.org/10.1038/s41467-019-13951-3.

(23) Wuister, S. F.; De Mello Donegá, C.; Meijerink, A. Influence of Thiol Capping on the Exciton Luminescence and Decay Kinetics of CdTe and CdSe Quantum Dots. *J. Phys. Chem. B* **2004**, *108* (45), 17393–17397. https://doi.org/10.1021/jp047078c.

(24) Kalyuzhny, G.; Murray, R. W. Ligand Effects on Optical Properties of CdSe Nanocrystals. *J. Phys. Chem. B* **2005**, *109* (15), 7012–7021. https://doi.org/10.1021/jp045352x.

(25) Bullen, C.; Mulvaney, P. The Effects of Chemisorption on the Luminescence of CdSe Quantum Dots. *Langmuir* **2006**, *22* (7), 3007–3013. https://doi.org/10.1021/la051898e.

(26) Munro, A. M.; Plante, I. J. La; Ng, M. S.; Ginger, D. S. Quantitative Study of the Effects of Surface Ligand Concentration on CdSe Nanocrystal Photoluminescence. *J. Phys. Chem. C* **2007**, *111* (17), 6220–6227. https://doi.org/10.1021/jp068733e.

(27) Koole, R.; Schapotschnikow, P.; de Mello Donegá, C.; Vlugt, T. J. H.; Meijerink, A. Time-Dependent Photoluminescence Spectroscopy as a Tool to Measure the Ligand Exchange

Kinetics on a Quantum Dot Surface. *ACS Nano* **2008**, *2* (8), 1703–1714. https://doi.org/10.1021/nn8003247.

(28) Deng, D.; Xia, J.; Cao, J.; Qu, L.; Tian, J.; Qian, Z.; Gu, Y.; Gu, Z. Forming Highly Fluorescent Near-Infrared Emitting PbS Quantum Dots in Water Using Glutathione as Surface-Modifying Molecule. *J. Colloid Interface Sci.* **2012**, *367* (1), 234–240. https://doi.org/10.1016/j.jcis.2011.09.043.

(29) Fischer, A.; Rollny, L.; Pan, J.; Carey, G. H.; Thon, S. M.; Hoogland, S.; Voznyy, O.; Zhitomirsky, D.; Kim, J. Y.; Bakr, O. M.; et al. Directly Deposited Quantum Dot Solids Using a Colloidally Stable Nanoparticle Ink. *Adv. Mater.* **2013**, *25* (40), 5742–5749. https://doi.org/10.1002/adma.201302147.

(30) Shestha, A.; Yin, Y.; Andersson, G. G.; Spooner, N. A.; Qiao, S.; Dai, S. Versatile PbS Quantum Dot Ligand Exchange Systems in the Presence of Pb-Thiolates. *Small* **2017**, *13* (5), 1–6. https://doi.org/10.1002/smll.201602956.

(31) Stern, H. L.; Musser, A. J.; Gelinas, S.; Parkinson, P.; Herz, L. M.; Bruzek, M. J.; Anthony, J.; Friend, R. H.; Walker, B. J. Identification of a Triplet Pair Intermediate in Singlet Exciton Fission in Solution. *Proc. Natl. Acad. Sci.* **2015**, *112* (25), 7656–7661. https://doi.org/10.1073/pnas.1503471112.

(32) Kroupa, D. M.; Arias, D. H.; Blackburn, J. L.; Carroll, G. M.; Granger, D. B.; Anthony, J. E.; Beard, M. C.; Johnson, J. C. Control of Energy Flow Dynamics between Tetracene Ligands and PbS Quantum Dots by Size Tuning and Ligand Coverage. *Nano Lett.* **2018**, *18* (2), 865–873. https://doi.org/10.1021/acs.nanolett.7b04144.

(33) Bender, J. A.; Raulerson, E. K.; Li, X.; Goldzak, T.; Xia, P.; Van Voorhis, T.; Tang, M. L.; Roberts, S. T. Surface States Mediate Triplet Energy Transfer in Nanocrystal-Acene

Composite Systems. *J. Am. Chem. Soc.* **2018**, *140* (24), 7543–7553. https://doi.org/10.1021/jacs.8b01966.

(34) Papa, C. M.; Garakyaraghi, S.; Granger, D. B.; Anthony, J. E.; Castellano, F. N. TIPS-Pentacene Triplet Exciton Generation on PbS Quantum Dots Results from Indriect Sensitization. *Chem. Sci.* **2020**, *11*, 5690–5696. https://doi.org/10.1039/D0SC00310G.

(35) Thompson, N. J.; Wilson, M. W. B.; Congreve, D. N.; Brown, P. R.; Scherer, J. M.; Bischof, T. S.; Wu, M.; Geva, N.; Welborn, M.; Voorhis, T. Van; et al. Energy Harvesting of Non-Emissive Triplet Excitons in Tetracene by Emissive PbS Nanocrystals. *Nat. Mater.* **2014**, *13* (11), 1039–1043. https://doi.org/10.1038/nmat4097.

(36) Hyun, B. R.; Zhong, Y. W.; Bartnik, A. C.; Sun, L.; Abruña, H. D.; Wise, F. W.; Goodreau, J. D.; Matthews, J. R.; Leslie, T. M.; Borrelli, N. F. Electron Injection from Colloidal PbS Quantum Dots into Titanium Dioxide Nanoparticles. *ACS Nano* **2008**, *2* (11), 2206–2212. https://doi.org/10.1021/nn800336b.

(37) Brown, P. R.; Kim, D.; Lunt, R. R.; Zhao, N.; Bawendi, M. G.; Grossman, J. C.; Bulović, V. Energy Level Modification in Lead Sulfide Quantum Dot Thin Films through Ligand Exchange. *ACS Nano* **2014**, *8* (6), 5863–5872. https://doi.org/10.1021/nn500897c.

(38) Chuang, C. H. M.; Brown, P. R.; Bulović, V.; Bawendi, M. G. Improved Performance and Stability in Quantum Dot Solar Cells through Band Alignment Engineering. *Nat. Mater.* **2014**, *13* (8), 796–801. https://doi.org/10.1038/nmat3984.

(39) Hu, L.; Wang, W.; Liu, H.; Peng, J.; Cao, H.; Shao, G.; Xia, Z.; Ma, W.; Tang, J. PbS Colloidal Quantum Dots as an Effective Hole Transporter for Planar Heterojunction Perovskite Solar Cells. *J. Mater. Chem. A* **2015**, *3* (2), 516–518. https://doi.org/10.1039/c4ta04272g.

(40) Garakyaraghi, S.; Mongin, C.; Granger, D. B.; Anthony, J. E.; Castellano, F. N. Delayed Molecular Triplet Generation from Energized Lead Sulfide Quantum Dots. *J. Phys. Chem. Lett.* **2017**, *8* (7), 1458–1463. https://doi.org/10.1021/acs.jpclett.7b00546.

(41) Valiev, M.; Bylaska, E. J.; Govind, N.; Kowalski, K.; Straatsma, T. P.; Van Dam, H. J. J.; Wang, D.; Nieplocha, J.; Apra, E.; Windus, T. L.; et al. NWChem: A Comprehensive and Scalable Open-Source Solution for Large Scale Molecular Simulations. *Comput. Phys. Commun.* **2010**, *181* (9), 1477–1489. https://doi.org/10.1016/j.cpc.2010.04.018.

(42) Knauf, R. R.; Lennox, J. C.; Dempsey, J. L. Quantifying Ligand Exchange Reactions at CdSe Nanocrystal Surfaces. *Chem. Mater.* **2016**, *28* (13), 4762–4770. https://doi.org/10.1021/acs.chemmater.6b01827.

Supporting Information for: Thiol Anchored TIPS-Tetracene Ligands with Quantitative Triplet Energy Transfer to PbS QDs and Improved Thermal Stability

Victor Gray†,‡, Zhilong Zhang†, Simon Dowland†, Jesse R. Allardice†, Antonios M. Alvertis†, James Xiao†, Neil Greenham†, John E. Anthony||, Akshay Rao†**

†Cavendish Laboratory, University of Cambridge, J. J. Thomson Avenue, Cambridge CB3 0HE, U.K.

‡Department of Chemistry - Ångström Laboratory, Uppsala University, Box 523, 751 20, Uppsala, Sweden.

||University of Kentucky Center for Applied Energy Research, 2582 Research Park Drive, Lexington Kentucky 40511, United States.

*corresponding author email: ar525@cam.ac.uk, anthony@uky.edu

Methods/Experimental

Chemicals

5,12-bis((triisopropylsilyl)ethynyltetracene (**TIPS-Tc**, Figure S1 left) was purchased from Ark Pharm. 6,11-bis((triisopropylsilyl)ethynyl)tetracene-2-carboxylic acid (**TET-CA**) was synthesized as described previously.[1] 6,11-bis((triisopropylsilyl)ethynyl) tetracene-2-methylthiol was synthesized as described below. All standard solvents were purchased in bulk from VWR or Sigma Aldrich. Anhydrous THF was purchased from Sigma Aldrich. All other chemicals were purchased from commercial sources and used as received unless otherwise noted. 4-methyl phthalaldehyde[2] and 1,4-dihydroxynaphthalene[1] were synthesized according to literature procedures. NMR spectra were measured on a 400 MHz Varian Unity spectrometer. Chemical shifts of each spectrum are reported in ppm and referenced to their corresponding deuterated solvents as listed. GC-MS was measured using a Bruker Scion-SQ GC-MS with an EI source. X-ray diffraction data were collected at low temperature on Bruker D8 Venture kappa-axis diffractometers using MoK(alpha) X-rays. Raw data were integrated, scaled, merged and corrected for Lorentz-polarization effects using the APEX3 (D8) program. Corrections for absorption were applied using SADABS.[3] Structures were solved by direct methods (SHELXT[4]) and refinements were carried out against F^2 by weighted full-matrix least-squares (SHELXL[5]). Hydrogen atoms were found in difference maps, but subsequently placed at idealized positions and refined using a riding model. Non-hydrogen atoms were refined with anisotropic displacement parameters. Atomic scattering factors were taken from the International Tables for Crystallography. Mass spectra were acquired on a Bruker Microflex LRF.

Synthesis

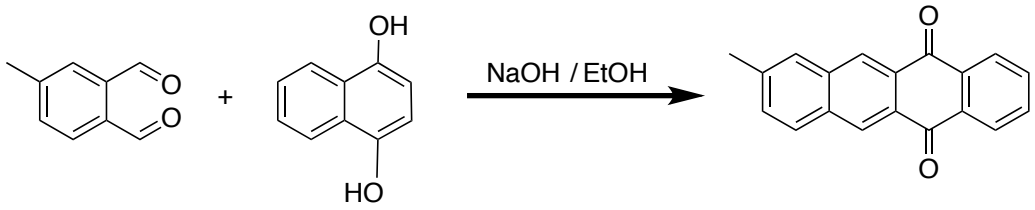

8-Methyl 5,12-naphthacenequinone: To a stirred solution of 4-methyl phthalaldehyde (2 grams, 13.5 mmol) and 1,4-dihydroxynaphthalene (2.16 g, 13.5 mmol) in 20 mL ethanol in a 125 mL Erlenmeyer flask was added 5 drops of a 15% aqueous solution of sodium hydroxide. Within 20 seconds, a brown precipitate of the desired quinone began to form, and the slurry was allowed to

stir for 4 hours. After that time, the suspension was filtered to collect the precipitate, which was washed first with methanol then ether, and then air dried to yeld 2.5 grams (9.2 mmol, 68%) of the desired quinone as a pale yellow, sparingly soluble powder. MS (LDI-MS, *e/z*): 272.08 (M^+, 100%).

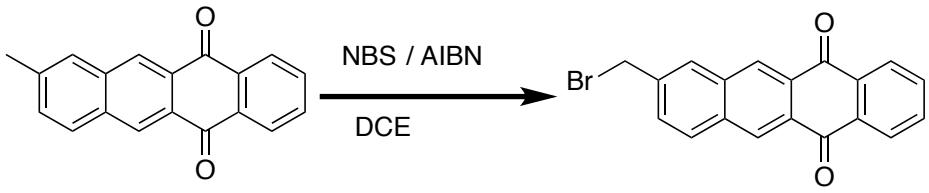

8-Bromomethyl 5,12-naphthacenequinone: A suspension of methyl naphthoquinone (2.15 g, 7.9 mmol) and N-Bromosuccinimide (1.55 g, 8.7 mmol) in 150 mL of 1,2-dichloroethane was heated to a *hard* reflux, at which point both solids had completely dissolved. Small amounts of AIBN were added periodically to this refluxing mixture until TLC analysis showed complete reaction of the starting material (approx. 5 hours). The *hot* solution was quickly filtered through a thin pad of silica gel, which was then flushed with dichloromethane until TLC showed all product had eluted. This solution was evaporated to yield crude bromomethyl naphthoquinone (2.16 g, 6.17 mmol, 71%) which was used directly in the next step.

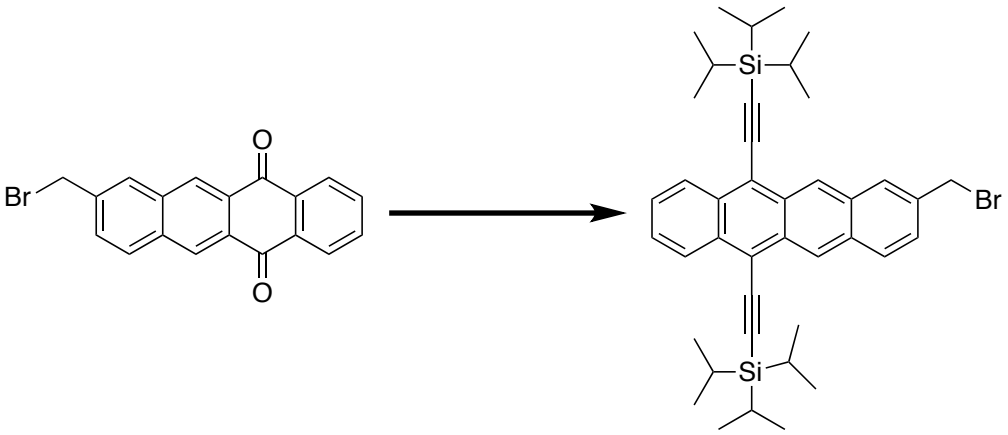

8-Bromomethyl-5,12-bis(triisopropylsilylethynyl) tetracene: To 100 mL of hexanes in a flame-dried, nitrogen-cooled round bottom flask with egg-shaped stir bar was added 1.55 mL (7 mmol) triisopropylsilyl acetylene, followed by 2.5 mL of 2.5 M n-BuLi in hexanes (6.25 mmol). After 1 hour stirring at room temperature, 0.8 g (2.3 mmol) of bromomethyl naphacenequinone was added in one portion, followed by 5 mL of anhydrous THF, and the solution was allowed to stir under nitrogen overnight. The next morning, 1 mL of sat. aq. ammonium chloride was added, followed by 2 g (10 mmol) of stannous chloride dehydrate, and 2 mL of 50% aqueous sulfuric acid. This mixture was allowed to stir for 1 hour. The solution was then poured into 200 mL hexanes, and extracted with 10% HCl, then exhaustively with water. The solution was then dried ($MgSO_4$) and passed through a thick plug of silica gel. The solvent was evaporated, and the resulting solid recrystallized from hexanes to yield the desired compound as deep red plates (1.14 g, 1.68 mmol, 73% - recrystallization solvent is incorporated into crystal). Structure was confirmed by X-ray crystallography. HRMS expected for $C_{41}H_{53}BrSi_2$: 680.2869. Found: 680.2871.

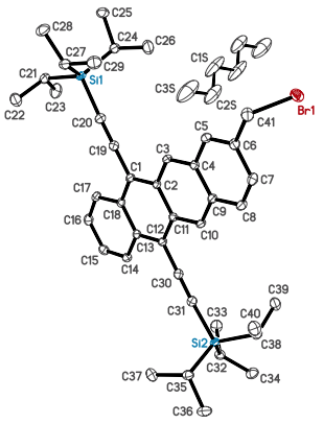

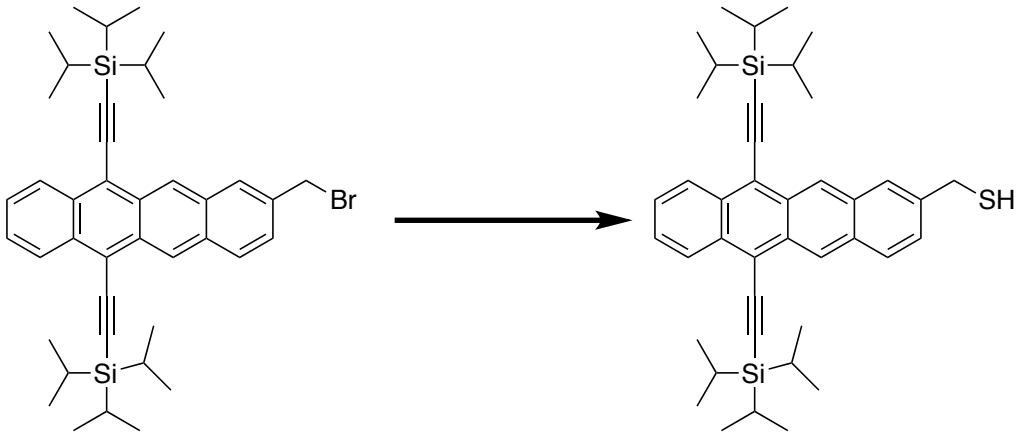

8-thiomethylene-5,12-bis(triisopropylsilylethynyl) tetracene: To 1.0 grams (1.5 mmol) bromomethyl TIPS tetracene was added 0.48 grams (1.5 mmol) tetrabutyl ammonium bromide. This solution was sparged with nitrogen to remove all traces of oxygen, then a degassed aqueous solution of sodium hydrosulfide (0.34 g, 6 mmol, in 5 mL water) was added, and the biphasic system stirred vigorously for 5 days. The layers were then separated, and the thiomethylene derivative was purified by chromatography on silica gel (hexanes / dichloromethane), followed by precipitation from 2-propanol to yield a deep orange solid (0.48 g, 0.75 mmol, 50%). HRMS calculated for $C_{41}H_{54}SSi_2$: 634.3485 Found: 634.3479.

Quantum dot synthesis and ligand exchange

Synthesis of PbS QDs was carried out following the procedure by Hines and Scholes with modifications.[6,7] In summary, PbO (0.45 g), oleic acid (1.6 - 14 g, depending on the targeted band

gap) and 1-octadecene (10 g) were degassed in a three-necked flask at 110°C for 2 h. The temperature was then reduced to 95°C. Under nitrogen, a solution of bis(trimethylsilyl)sulphide (210 µL) in 1-octadecene (5 mL) was rapidly injected into the lead precursor solution. After cooling naturally to room temperature the PbS QDs were washed 4 times by precipitation/re-dispersion with acetone and hexane. The purified QDs were stored in a nitrogen filled glovebox at high concentration (>40 mg/mL / >100 µM) until use.

Ligand exchange was carried out under nitrogen. QDs in toluene were diluted to 42 µM in a Toluene/THF mixture of 4:1. The ligand in 100 mg/mL THF solutions was added to the QD solution, keeping a ligand to QD mass ratio of 1:2 for all sizes of QDs. Ligand coverage and size distribution is summarized in Table S1. Coverage of **TET-CA** and dot characteristics has been reported previously.[8]

Table S1. Properties of the synthesized PbS QDs and ligand coverages.

Exciton Bandgap (eV)	Diameter (nm)	Size Distribution[a] (%)	**TET-CA** Ligand/QD	**TET-CA** Ligand/nm^2	**TET-SH** Ligand/QD	**TET-SH** Ligand/nm^2
0.90	4.9	5.3	37.0	0.47	-	-
1.00	4.3	8.0	34.0	0.57	25.0	0.52
1.08	4.0	6.3	25.6	0.53	23.4	0.49
1.18	3.5	8.2	24.5	0.63	18.0	0.47
1.30	3.1	4.9	20.8	0.69	16.9	0.56

[a]size distribution = standard deviation/mean size x 100%.[9]

Ligand Coverage

The ligand coverage was determined form UV-Vis absorption. The concentration of the PbS QD was estimated using the empirical formula for the molar absorptivity by Moreels *et al*.[10] The molar absorption coefficient of the **TET-SH** ligand was assumed to be the same as the **TET-CA** ligand, 25500 $M^{-1}cm^{-1}$ at the peak absorption in toluene.[8]

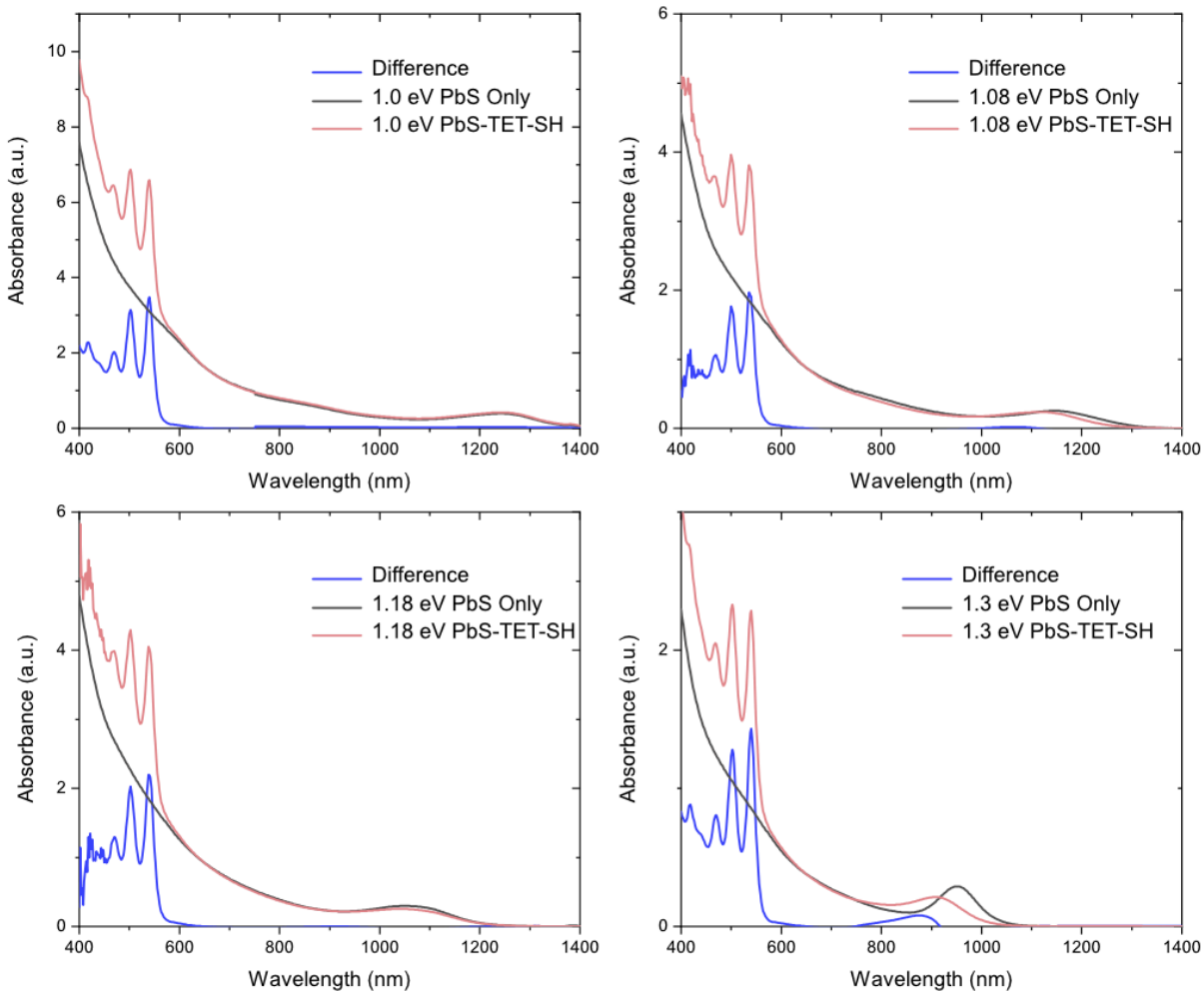

*Figure S5. Absorption spectra of PbS QDs and PbS QDs with **TET-SH** ligand in toluene, used to determine the ligand coverage.*

Optical spectroscopy

Steady-state absorption

A Shimadzu UV3600Plus spectrometer was used to measure the absorbance spectra of the solutions. The high concentration of the PM solutions required samples to be measured in rectangular capillary tubes with a 200 µm pathlength.

PLQE

The integrating sphere and PLQE measurement procedure has been described previously.[11,12] An integrating sphere with a Spectralon-coated interior (Newport 819C-SL-5.3) was used for the absolute measurement. 515 nm and 658 nm laser diodes (Thorlabs) with a beam diameter at the sample of 3 mm was used as the excitation source. Light from the sphere was coupled into an Andor Kymera 328i Spetrograph equipped with an InGaAs detector (Andor, iDus InGaAs 490). A NIST certified calibration lamp from Newport (63355 200W Quartz Tungsten Halogen Lamp), driven by an OPS-Q250 power supply was used to generate a photons/count calibration file. The calibration file was generated by producing an irised beam of light from the calibration source into the integrating sphere, the spectral response was recorded with and without a series of long-pass

filters in order to resolve the longer wavelength response absent of the second harmonics from the shorter wavelengths, these were then also corrected for by measuring the transmission spectra of the filters. The calibration file was generated by comparing this data set to the calibrated spectrum of the lamp. To validate the calibration, a Rhodamine 6G sample in ethanol was measured in the sphere with 520 nm excitation. Three spectra were taken, with laser excitation on and off the sample and a blank sample. Each recorded spectra was multiplied with the generated correction curve to obtain the corrected spectra. From the corrected spectra the PLQE was calculated to 92-95 %, in good agreement with literature.[13]

Cyclic Voltammetry

Cyclic voltammetry was performed on **TIPS-Tc** in an acetonitrile/toluene (1:4) mixture with $TBAPF_6$ (0.1 M) as electrolyte at a scan rate of 100 mV/s. 5 mM ferrocene was used as internal standard. A glassy carbon electrode was used as working electrode, a Pt wire as counter electrode and a $Ag/AgNO_3$ reference electrode.

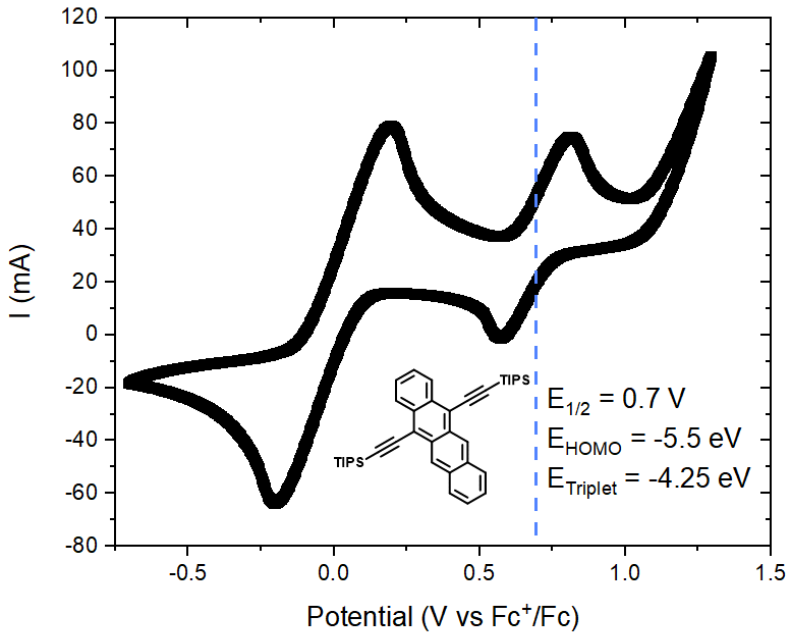

*Figure S6. Cyclic voltammogram of **TIPS-Tc** in Acetonitrile/Toluene (1:4), 0.1M $TBAPF_6$ as electrolyte and 5mM ferrocene as internal standard. Determined oxidation potential, HOMO level and Triplet level.*

Photoluminescence Spectra

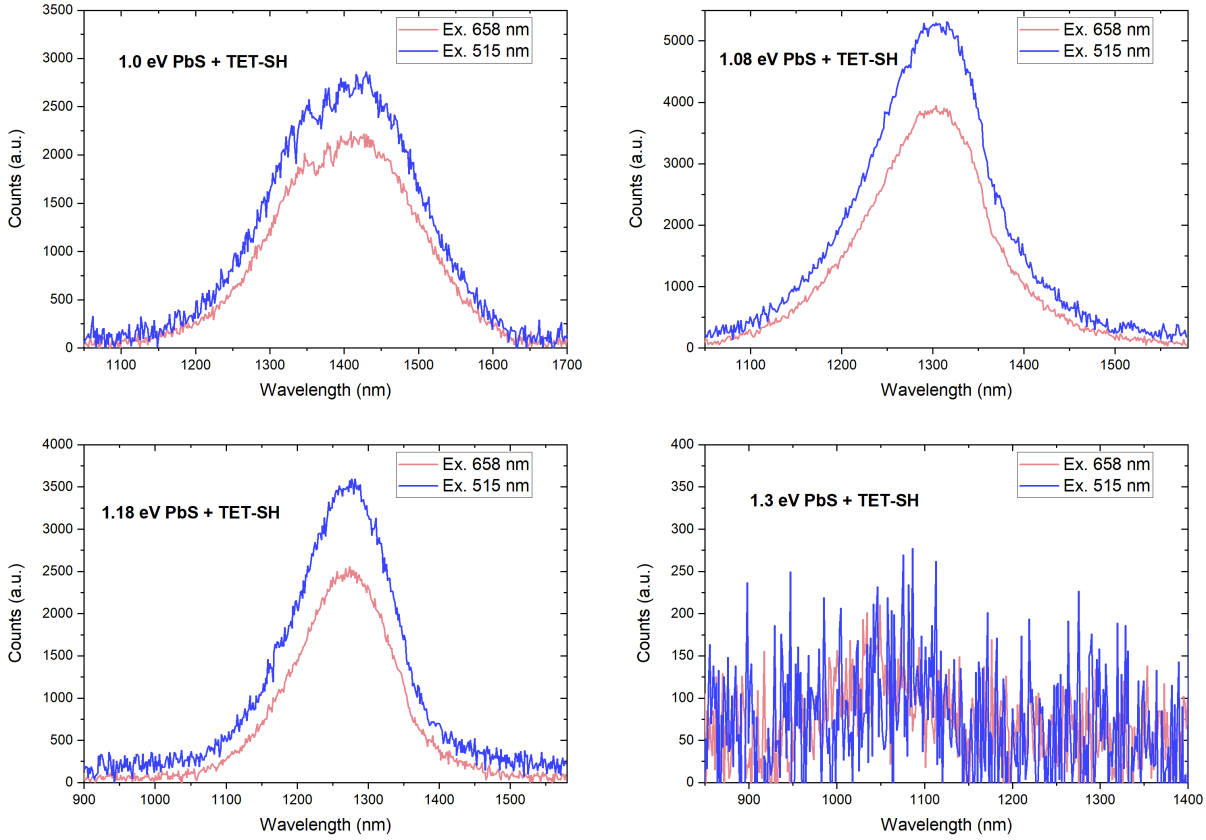

*Figure S7. Photoluminescence spectra of PbS quantum dots of different bandgap after ligand exchange to **TET-SH** in a toluene solution with 200 mg/mL **TIPS-Tc**, exciting the QDs directly (658 nm) or the singlet fission material **TIPS-Tc** (515 nm). QD concentrations are 0.2 mM.*

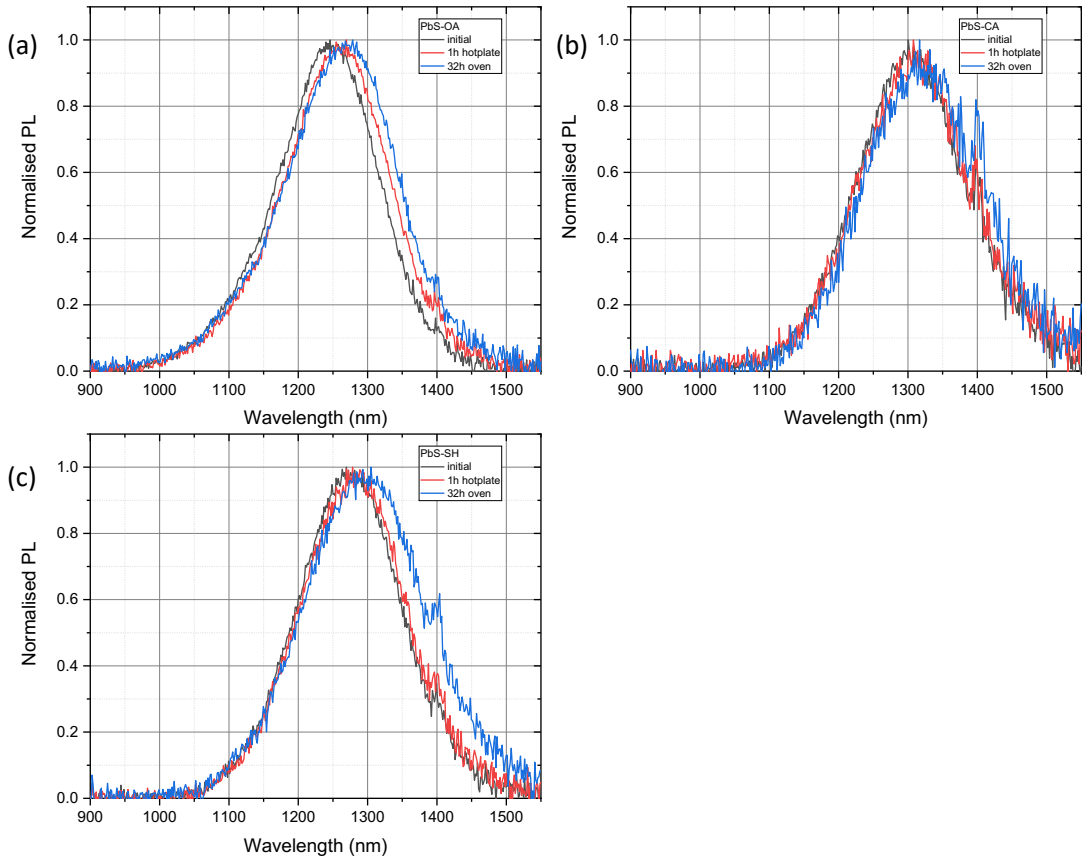

*Figure S8. Photoluminescence spectra of PbS QDs capped with oleic acid, **TET-CA** or **TET-SH** ligands in toluene, before and after heating the samples to 100 °C for 1 h and 32h.*

References

(1) Kroupa, D. M.; Arias, D. H.; Blackburn, J. L.; Carroll, G. M.; Granger, D. B.; Anthony, J. E.; Beard, M. C.; Johnson, J. C. Control of Energy Flow Dynamics between Tetracene Ligands and PbS Quantum Dots by Size Tuning and Ligand Coverage. *Nano Lett.* **2018**, *18*, 865–873.

(2) Farooq, O. Oxidation of Aromatic 1,2-Dimethanols by Activated Dimethyl Sulfoxide. *Synthesis (Stuttg).* **1994**, 1035–1036.

(3) Krause, L.; Herbst-Irmer, R.; Sheldrick, G. M.; Stalke, D. Comparison of Silver and Molybdenum Microfocus X-Ray Sources for Single-Crystal Structure Determination. *J. Appl. Crystallogr.* **2015**, *48*, 3–10.

(4) Sheldrick, G. M. SHELXT - Integrated Space-Group and Crystal-Structure Determination. *Acta Crystallogr. Sect. A Found. Crystallogr.* **2015**, *71*, 3–8.

(5) Sheldrick, G. M. Crystal Structure Refinement with SHELXL. *Acta Crystallogr. Sect. C Struct. Chem.* **2015**, *71*, 3–8.

(6) Hines, M. A.; Scholes, G. D. Colloidal PbS Nanocrystals with Size-Tunable Near-Infrared Emission: Observation of Post-Synthesis Self-Narrowing of the Particle Size Distribution. *Adv. Mater.* **2003**, *15*, 1844–1849.

(7) Zhang, J.; Crisp, R. W.; Gao, J.; Kroupa, D. M.; Beard, M. C.; Luther, J. M. Synthetic Conditions for High-Accuracy Size Control of PbS Quantum Dots. *J. Phys. Chem. Lett.* **2015**, *6*, 1830–1833.

(8) Gray, V.; R. Allardice, J.; Zhang, Z.; Dowland, S.; Xiao, J.; J. Petty, A.; E. Anthony, J.; C. Greenham, N.; Rao, A. Direct vs Delayed Triplet Energy Transfer from Organic Semiconductors to Quantum Dots and Implications for Luminescent Harvesting of Triplet Excitons. *ACS Nano* **2020**, 10.1021/acsnano.9b09339.

(9) Zhang, J.; Gao, J.; Miller, E. M.; Luther, J. M.; Beard, M. C. Diffusion-Controlled Synthesis of PbS and PbSe Quantum Dots with in Situ Halide Passivation for Quantum Dot Solar Cells. *ACS Nano* **2014**, *8*, 614–622.

(10) Moreels, I.; Lambert, K.; Muynck, D. De; Vanhaecke, F.; Poelman, D.; Martins, J. C.; Allan, G.; Hens, Z. Size-Dependent Optical Properties of Colloidal PbS Quantum Dots. *ACS Nano* **2009**, *3*, 3023–3030.

(11) De Mello, J. C.; Wittmann, H. F.; Friend, R. H. An Improved Experimental Determination of External Photoluminescence Quantum Efficiency. *Adv. Mater.* **1997**, *9*, 230–232.

(12) Allardice, J. R.; Thampi, A.; Dowland, S.; Xiao, J.; Gray, V.; Zhang, Z.; Budden, P.; Petty, A. J.; Davis, N. J. L. K.; Greenham, N. C.; Anthony, J. E.; Rao, A. Engineering Molecular Ligand Shells on Quantum Dots for Quantitative Harvesting of Triplet Excitons Generated by Singlet Fission. *J. Am. Chem. Soc.* **2019**, *141*, 12907–12915.

(13) Kubin, R. F.; Fletcher, A. N. Fluorescence Quantum Yields of Some Rhodamine Dyes. *J. Lumin.* **1982**, *27*, 455–462.